A novel prognostic six-CpG signature in glioblastomas

An-An Yin, Nan Lu, Amandine Etcheverry, Marc Aubry, Jill Barnholtz-Sloan, Lu-Hua Zhang, Jean Mosser, Wei Zhang, Xiang Zhang, Yu-He Liu, et al.

A novel prognostic six-CpGs signature in glioblastomas

An-An Yin [1, 2], Nan Lu [1,3], Amandine Etcheverry [4,5,6], Marc Aubry [5, 7], Jill Barnholtz-Sloan [8], Lu-Hua Zhang [9], Jean Mosser [2,3,4,5], Wei Zhang [2], Xiang Zhang [2] Yu-He Liu [1], Ya-Long He [2]

[1] Department of Neurosurgery, The 88th Hospital of the People's Liberation Army, Taian, Shandong Province, The People's Republic of China

[2] Department of Neurosurgery, Xijing Institute of Clinical Neuroscience, Xijing Hospital, Air Force Military Medical University, Xi'an, Shaanxi Province, The People's Republic of China

[3] Department of Neurosurgery, Changhai Hospital, Navy Military Medical University, Shanghai, The People's Republic of China

[4] CNRS, UMR 6290, Institut de Génétique et Développement de Rennes (IGdR), Rennes F-35043, France

[5] Université Rennes1, UEB, UMS 3480 Biosit, Faculté de Médecine, Rennes F-35043, France

[6] CHU Rennes, Service de Génétique Moléculaire et Génomique, Rennes F-35033, France

[7] Plate-forme Génomique Santé Biosit, Université Rennes1, Rennes F-35043, France

[8] Case Comprehensive Cancer Center, Case Western Reserve University, Cleveland, Ohio, United States of America

[9] Department of Neurosurgery, No. 425 Hospital of the People's Liberation Army, San Ya, Hainan Province, The People's Republic of China

The first three authors contribute equally to this work

Correspondence authors: Yu-He Liu (email: lyhws@sina.com) at The department of neurosurgery, the 88th Hospital of the People's Liberation Army, Huanshang Road,

No. 217, Taian, Shandong Province, 271000, The People's Republic of China Tel.: +86 538 8839302, and Ya-Long He (email: heyl.fmmu@hotmail.com) at Department of Neurosurgery, Xijing Institute of Clinical Neuroscience, Xijing Hospital, Air Force Military Medical University, Changle West Road, No. 169, Xi'an, Shaanxi Province 710032, the People's Republic of China. Tel.: +86 29 84771323; fax: +86 29 84775567

Key words: Glioblastomas; Bevacizumab; DNA methylation; Risk-score signature; Prognostication;

Running title: Novel Epigenetic Signature in GBMs

Compliance with Ethical Standards

Ethical approval: All procedures performed in studies involving human were in accordance with the ethical standards of the institutional research committee of Rennes and Angers University Hospitals (France) and with the 1964 Helsinki declaration and its later amendments or comparable ethical standards

Informed consent: Informed consent was obtained from all participants from the Neurosurgery Departments of Rennes and Angers University Hospitals

Consent for publication: Not applicable

Disclosure of Potential Conflicts of Interest: No potential conflicts of interest were disclosed

Abbreviations:

GBM=glioblastoma

OS=overall survival

PFS=progression-free survival

G-CIMP=glioma-CpGs island methylator phenotype

CGI=CpGs island

MGMT=the O-6-methylguanine-DNA methyltransferase

RT=radiation

TMZ=temozolomide

GSEA=gene set enrichment analysis

Author contributions

A. Yin, N. Lu, A. Etcheverry, J. Mosser and Y. He designed the study; A. Yin, N. Lu, A. Etcheverry, interpreted the data and wrote the paper; A. Etcheverry, M. Aubry, J. Barnholtz-Sloan, and J. Mosser generated microarray data; Y. He and L. Zhang in revised the paper; J. Mosser, Y. He and Y. Liu supervised the entire study.

Abstract

Aims: We aimed to identify a clinically useful biomarker using DNA methylation-based information to optimize individual treatment of glioblastoma (GBM) patients.

Methods: A six-CpGs panel was identified by incorporating genome-wide DNA methylation data and clinical information of three distinct discovery sets, and was combined using a risk-score model. Different validation sets of GBMs and lower-grade gliomas and different statistical methods were implemented for prognostic

evaluation. An integrative analysis of multi-dimensional TCGA data was performed to molecularly characterize different risk tumors.

Results: The six-CpGs risk score signature robustly predicted overall survival (OS) in all discovery and validation cohorts, and in a treatment-independent manner. It also predicted progression-free survival (PFS) in available patients. The multi-maker epigenetic signature was demonstrated as an independent prognosticator, and had better performance than known molecular indicators such as glioma-CpGs island methylator phenotype (G-CIMP) and proneural subtype. The defined risk subgroups were molecularly distinct; high-risk tumors were biologically more aggressive with concordant activation of pro-angiogeneic signaling at multi-molecular levels. Accordingly we observed better OS benefits of bevacizumab-contained therapy to high-risk patients in independent sets, supporting its implication in guiding usage of anti-angiogeneic therapy. Finally the six-CpGs signature refined the risk classification based on G-CIMP and *MGMT* methylation status.

Conclusions: The novel six-CpGs signature is a robust and independent prognostic indicator for GBMs and is of promising value to improve personalized management.

Introduction

Glioblastomas (GBMs) are the most frequent and vicious subtype of all gliomas [1, 2]. Molecular and clinical heterogeneity critically hindered better treatment outcomes for this deadly disease. The development of clinical informative biomarkers would be helpful for improving the current management of GBMs.

DNA methylation marks have long been the leading candidates for cancer biomarker discovery [3]. Human cancers including GBMs were commonly developed with global hypomethylation of gene-poor DNA repeats and large hypomethylated blocks of gene regions concurrent with relevant CpGs island (CGI) hypermethylation [4]. Those epigenetic abnormalities played crucial roles in determining tumor phenotypic behaviors via regulating gene expression and chromatin organization [5]. Early studies with candidate-gene approaches have identified numerous DNA methylation alterations in key genes (e.g., *TIMP3*, *RASSF1A*, and *p16INK4a*) with potential clinical values for GBMs [6]. Promoter methylation status of the O-6-methylguanine-DNA methyltransferase (*MGMT*), encoding a DNA repair enzyme that confers resistance to alkylating agents, represented the most promising one with robust predictive ability for temozolomide (TMZ) outcome [7]. Unfortunately, the single-gene based epigenetic biomarkers including *MGMT* had limited roles in guiding clinical decision, and failed to warrant a change in routine testing [7]. In recent years, there have been an increasing number of high-throughput techniques devoted to accomplishing genome-wide assessment of cancer epigenomes [4, 5, 8]. The application of those latest approaches may be helpful for identifying more powerful biomarkers based on multi-marker epigenetic signatures.

In this study, by integrating genome-wide DNA methylation microarray data and clinical information, we reported a novel biologically relevant six-CpGs signature for

GBMs. The signature robustly predicted survival of GBM patients in a treatment-independent manner, and was of promising value to improve current patient management.

Materials and Methods

Patient cohorts

Seventy-nine adult patients (aged ≥18 years old) with newly diagnosed GBMs were collected between 2004 and 2013 from the Neurosurgery Departments of Rennes and Angers University Hospitals (***RAUH_450k***). Initial histological diagnoses were confirmed by a central review panel including at least two neuropathologists. All patients were homogenously treated with Stupp regimen [9]. The median follow-up period was 53 months, with a range of 8 to 113 months [10]. Snap-frozen samples were collected at the time of surgery, following informed consent, in accordance with the French regulations and the Helsinki Declaration. DNA was extracted using the NucleoSpin TissueKit (Macherey Nagel). The quality of DNA samples was assessed by electrophoresis in a 1% agarose gel. DNA methylation profiling was performed by the Infinium HumanMethylation450k platform (Illumina Inc.) according to the manufacturer's instructions. Image processing and intensity data extraction were performed within Genome Studio (Illumina Inc.).The novel BMIQ (Beta MIxture Quantile dilation) algorithm was used for intra-array normalization [11]. Methylation level of each CpGslocus is summarized as β value, ranging from 0 (completely unmethylated) to 1 (completely methylated). Methylation data have been submitted in The ArrayExpress under accession number "E-MTAB-4969".

A published cohort of fifty GBMs and three non-tumor brains (NBs) from the Neurosurgery Departments of Rennes and Angers University Hospitals was also

included (GSE22867; ***RAUH_27k***) [12], with microarray data by Infinium27k platform (Illumina Inc.).

Public GBM datasets with DNA methylation data were obtained from The Cancer Genome Atlas (TCGA) including ***TCGA_27k*** (GBMs, n=282; NBs, n=4) and ***TCGA_450k*** (GBMs, n=113) [13]; from Chinese Glioma Genome Atlas (CGGA) (***CGGA_27k***; GBMs, n=30) [14]; and from the Gene Expression Omnibus (GEO) repository including ***GSE50923_27k*** (GBMs, n=54; NBs, n=24) [15], ***GSE60274_450k*** (GBMs, n=64; NBs, n=5) [16] and ***GSE36278_450k*** (GBMs, n=57; tumors harboring mutations in *H3F3A* and those from TCGA were excluded) [17]. Patient characteristics of the included GBM datasets were summarized in Table 1. Molecular datasets of lower-grade gliomas (LGG, grade II to III) were also used for additional validation, including ***TCGA-LGG_450k*** (n=482), ***CGGA-LGG_27k*** (n=109), and ***GSE48462_450k*** (n=117). All NBs were obtained from apparently healthy individuals or chronic epilepsy patients without pathological evidence of other neurological or psychiatric diseases in each dataset. Among the datasets with gliomas of all grades and ages, only those aged ≥ 18 years old, and with a histological diagnosis of GBMs, were included in this study, and patients with a follow-up time ≥ one month were kept for survival analysis.

Probe selection and risk-score model construction

Prior probe selection was performed by removing those not interrogated on both platforms, those targeting the sex chromosomes, those containing a single-nucleotide polymorphism (SNP) within five base pairs of the probes, and those not annotated with any protein-coding or non-protein-coding genes. Finally 21248 CpGs were kept for analysis. Differentially methylated CpGs were computed by two-sample wilcoxon sum rank test (*samr* R package). GBM-specific CpGs were defined as those having a

median β difference ≥ 0.2 between tumors and controls, and a false discovery rate (FDR) q-value ≤ 0.05. Correlation of DNA methylation with OS was evaluated by univariate Cox regression analysis with permutation test by Biometric Research Branch (BRB)-Array Tools. Prognostic CpGs were those with a permutation p value ≤ 0.05. Batch effects between each platform and dataset were adjusted by M-value transformation and the empirical Bayes approach (*ber* R package) [18, 19]. Missing β values were imputed by *impute* R package. The discovery-validation approach was employed to develop a risk-score model which is the sum of the methylation levels of each CpGs weighted by their univariate Cox coefficients (Figure 1a). The discovery phase was performed in TCGA_27k, RAUH_27k and GSE50923_27k. Cox coefficients were calculated from RAUH_27k; optimal cutoff for stratifying low-risk and high-risk tumors was determined by *maxstat* R package from all the discovery sets [20]. The validation phase was performed in five GBM cohorts and two LGG cohorts. The risk-score signature was also assessed with PFS outcome.

Indirect validation based on differential gene expression prediction

To add another layer of prognostic validation, we used the Support Vector Machines (SVM) model based on the differential expressed genes (4201 genes) between each risk subgroups from TCGA_27k, to predict the risk classification of our 6-CpGs signature. The prediction accuracy rate of the SVM model was 87% in TCGA_27k. Public gene expression datasets of GBMs were downloaded for indirect validation, including ***REMBRANDT*** (the Repository of Molecular Brain Neoplasia Data, n=181) [21], and ***GSE16011*** (n=147) [22].

Bioinformatic analysis

To gain biologically insightful view of the risk-score signature, an integrative analysis of multi-dimensional molecular data was performed within TCGA samples; 1) level 3

gene expression data from the Agilent G4502A Microarray (n=386) were analyzed by gene set enrichment analysis (GSEA) to evaluate the functional profiles between the risk subgroups on the gene sets of Gene Ontology Biological Processes and Kyoto Encyclopedia of Genes and Genomes (KEGG) from The Molecular Signatures Database (MSigDB) [23]; 2) level 3 copy number data from Affymetrix Genome-Wide Human SNP6.0 Array (n=382) were analyzed by GISTIC2.0 with amplitude threshold being ± 0.2 [24]; 3) level 2 somatic mutation data from Whole Exome sequencing (n=245) were analyzed by MutSigCV to identify significantly mutated genes, with a FDR q-value $\leqslant$ 0.05 being significant; and 4) level 3 microRNA data from Agilent 8x15K Human miRNA-specific Microarray (n=386) and level 3 protein data from Reverse Phase Protein Array (n=171) were both computed by two-sample t test to identify differentially expressed targets, with confidence level of FDR assessment = 80% and maximum allowed proportion of false-positive genes = 0.1. The DNA methylation clusters were determined by k-means (k=3) clustering on the 1503 probes reported by Noushmehr et al [25]. The gene expression subtypes were predicted using the Binary tree classification on expression data of the 840 classifiers reported by Verhaak et al [26]. *MGMT* promoter methylation status was determined using a logistic regression model based on two probes, i.e., cg12434587 and cg12981137 [27].

Statistical analysis

Hierarchical clustering analysis was performed within GenePattern. The distribution of molecular features with respect to each risk subgroup was tested by Fisher's exact test or Chi-square test. Overall survival (OS) was defined as the interval from the date of diagnosis to the date of death or last follow-up; progression-free survival (PFS) was the interval to the date of progression according to clinical and imaging criteria

[28], or to the date of death or last follow-up without progression. Survival data were estimated by the Kaplan-Meier Method, and compared by log-rank test. Univariate and multivariate Cox regression models were used to evaluate the correlation and independence of potential prognosticators. Meta-analysis was done by the inverse-variance method where application of either fixed- or random effect models was based on the statistical heterogeneity, with p-value for Chi-square test ≤ 0.05 for significance. The prognostic performance was evaluated by time-dependent receiver operating characteristic (ROC) curve (*survcomp* R package) [29]. Interaction analysis was conducted between the risk subgroups and paired treatments. All the calculations were done within SPSS Statistics and R software and P values ≤ 0.05 for significance were used.

Results

Identification of a novel GBM-specific six-CpGs panel for risk-score modeling

GBM-specific CpGs were respectively calculated from RAUH_27k, TCGA_27k, and GSE50923_27k (Figure 1a and Supplementary Table 1). Given the limitations in computing differential methylation for GBMs in each dataset (e.g., a few number of NB samples, non-matched controls, and inability for adjusting age and brain location), we used the overlap of 508 CpGs from all discovery sets to generate a representative list. Hierarchical clustering on the 508-CpGs signature accurately distinguished GBMs from NBs in two discovery sets and an independent validation cohort with only five tumors (1.8% of 168) being misclassified into the NB group, supporting the robustness of the list as differential methylation for GBMs (Figure 1b). Then by correlating methylation levels with OS, we identified an overlap of seven CpGs with high prognostic value (permutation $p \leq 0.05$) from the discovery sets. A panel of six CpGs with highly variable methylation patterns across tumors (standard deviation of β

value ≥ 0.15) was used for risk-score modeling (Figure 1c). Among the panel, two CpGs were from CGIs and hypermethyated while the others were outside CGI and hypomethylated in GBMs. The two CGI CpGs were regarded as risky for prognosis as their DNA methylation levels showed inverse correlation with OS; the four open sea CpGs were all protective with a positive correlation (Figure 1c). Moreover, four locus-related genes were associated with epigenetic silencing (*TRIM58* and *ADRA2C*) or re-expression (*TRIM38* and *MS4A7*) in GBMs (Figure 1d). In addition, despite not associating with differential expression status in GBMs (*HPD* and *SPNS3*), two open sea CpGs were essential for optimal prognostication as indicated by additional analyses (Supplementary Figure 1 and Table 2). Collectively the risk-score formula was constructed as follows: risk score = (2.333 × β value of cg07533148) + (1.508 × β value of cg10235817) + (-2.483 × β value of cg22502502) + (-2.573 × β value of cg02506908) + (-2.580 × β value of cg18343292) + (-3.031 × β value of cg18750756), with the optimal cutoff of -2.485 (around the 20^{th} percentile risk value from the discovery cohorts) for stratifying low-risk and high-risk patients (Figure 1a).

The prognostic value of the six-CpGs signature in the discovery and independent validation cohorts

Patients were divided to low-risk groups (with lower risk scores) and high-risk groups (with higher risk scores) in the discovery cohorts, where low-risk patients were consistently associated with longer OS than high-risk ones (Figure 2a). The epigenetic signature had been further validated in five independent validation cohorts of heterogeneous population; it accurately predicted OS not only for patients with combined radiation (RT) and TMZ but also for those with heterogeneous or unknown treatments (Figure 2b). Moreover, risk classification on differential gene expression profiles yielded significant OS difference between the predicted low-risk and high-

risk subgroups in REMBRANDT and GSE16011 (Supplementary Figure 2). Finally, the six-CpG signature was successfully validated in different datasets of LGGs and in particular the subtype with wide-type *IDH* and intact chromosome 1p/19q, which is reported be molecularly resembled with GBMs (Supplementary Figure 3) [30]. The six-CpG signature also predicted PFS in available GBM cohorts (Supplementary Figure 4).

The six-CpGs signature was an independent and superior prognostic factor for GBMs

Within all RAUH samples (27k and 450k collectively), univariate Cox regression model revealed that age, *MGMT* promoter methylation status, and the six-CpG signature were significantly correlated with OS (Table 2). Multivariate Cox model further demonstrated that the six-CpGs signature was an independent prognostic indicator (Table 2). Cox regression analyses yielded similar results with all TCGA patients (Table 2). The consistent prognostic value in stratified cohorts by different treatments supported that the six-CpGs signature was not a predictive indicator for specific treatment, but a prognostic factor for GBMs, which provides information on the likely outcome of cancer diseases independent of treatment (Supplementary Figure 5).

Time-dependent ROC analysis reported that the six-CpGs signature was associated with larger area under the curve (AUC) values than G-CIMP+ and proneural subtype at each time point, suggesting its superiority in survival prediction (Supplementary Figure 6). In addition, among patients treated with RT/TMZ, the six-CpGs signature and *MGMT* methylation status showed similar integrated AUC values, but had distinct evolution with respect to time; *MGMT* status and the six-CpGs signature respectively had larger AUC values at earlier and later time points (Supplementary Figure 6). This

finding suggested a possibility of the combination of the two indicators for optimal prognostication.

Molecular characterization of the six-CpGs signature using TCGA data

Correlation with established molecular subgroups showed that the low-risk group included all C-GIMP+ tumors and was enriched with proneural subtypes whilst the high-risk group was enriched with DNA methylation cluster#2 tumors described by Noushmehr et al. [25] and classical and mesenchymal subtypes (Figure 3a). Secondary GBMs were enriched in the low-risk group (Figure 3a). The risk subgroups were also associated with different ages even after excluding patients with C-GIMP+ tumors, which were known for younger ages at diagnosis (mean ages for G-CIMP- low-risk vs. high-risk tumors: 54.0 vs. 61.6 years old, $P<0.0001$). Somatic copy number variation (SCNV) analysis showed that the risk subgroups were associated with distinct chromosomal alterations: gain of Chr.7, Chr.19 and Chr.20 and loss of Chr.7 were more frequently seen in high-risk tumors (Figure 3a and Supplementary Figure 7). We also found that high-risk tumors harbored more significantly regional SCNVs (Supplementary Figure 7). Accordingly, at gene level, high-risk tumors were associated with more SCNVs in known cancer genes such as *EGFR*, *PDGFA*, *PTEN* and *CDNK2A/B* (Figure 3a). Somatic mutation analysis showed that the significantly mutated genes were much more in high-risk vs. low-risk tumors (227 vs. 11; Supplementary Table 3), among which mutations in *EGFR*, *COL6A3*, *PFAS*, and *WDR92* were more frequently seen in high-risk tumors whilst mutations in *TP53*, *ATRX*, and *IDH1* were enriched in low-risk tumors (Figure 3a). Of note, despite that some of the observed features (e.g., secondary cases, SCNVs in chr20, and mutations in *TP53*, *ATRX* and *IDH1*) were exclusively attributed to the enrichment of G-CIMP+

tumors in the low-risk group, the majority remained significant in the comparison of G-CIMP- low-risk and high-risk cases (Figure 3a).

As for functional profiles, GSEA on transcriptome data showed that low-risk tumors were enriched in signatures relating to normal brain function and developmental process whilst high-risk tumors were enriched with cancer-promoting signatures relating to immune response, NF-κB activation, apoptosis and angiogenesis (Figure 3b and Supplementary Table 4). Consistent with transcriptome data, the risk subgroups were also associated with distinct functional profiles at microRNAs and protein levels, among which high-risk tumors was mostly featured by elevation of pro-angiogeneic signaling (Supplementary Figure 8).

Potential links to differential outcomes of bevacizumab therapy

The multi-platform molecular profiling revealed concordant activation of pro-angiogenic signaling in high-risk tumors, and thus suggested possible better outcomes for anti-angiogneic therapy in this subgroup. We observed that, among TCGA patients who were treated with combined RT/TMZ, the utility of bevacizumab (either first-line or at progression; a humanized monoclonal antibody against VEGFA [31, 32]) did confer a clear OS benefit to high-risk patients, but was associated with similar outcome in the low-risk group (Figure 3b). Similar benefits were also observed in two independent sets on bevaicuzmab at progression (Figure 3b). Meta-analysis confirmed the significant differential outcomes by bevacizumab-contained therapy within each risk subgroup (test for subgroup differences, P=0.03; Figure 3d). Gehan-Breslow-Wilcoxon test further indicated that bevacizumab-contained therapy may be more useful for improving shorter-term survival for high-risk patients (Figure 3a).

The six-CpGs signature in stratified cohorts by known epigenetic markers

We also tested the prognostic interrelationship of the six-CpGs signature with known epigenetic indicators. Despite the enrichment of favorable G-CIMP+ tumors in the low-risk groups, the six-CpGs signature still showed great discriminating value for prognosis in the majority of GBMs without G-CIMP (Figure 4a and Supplementary Figure 9a).

As encouraged by time-dependent ROC analysis, we also employed the combination of the six-CpGs signature and *MGMT* methylation status to stratify patients who were treated with RT and TMZ, which yielded four distinct subgroups; patients with low-risk and *MGMT* methylated tumors had the best OS, followed by two subgroups with only one favorable mark, whilst those with high-risk and unmethylated tumors had the worst survival (Figure 4b and Supplementary Figure 9b).

Finally, time-dependent ROC analysis confirmed the refined risk classification with the addition of our signature (Supplementary Figure 6).

Discussion

Clinically informative biomarkers played crucial roles in precision oncology [33]. Historically, RNA- or protein-based information had been the mainstream for biomarker discovery, and indeed brought clinical benefits to cancer patients [3]. However, the expression-based biomarkers had critical drawbacks for clinical utility – the information provided was unstable and sometimes misleading due to the highly dynamic nature of RNAs and proteins in cancer biology and the vulnerable physic-chemical nature in biological specimens [3]. In this respect, DNA methylation-based information was much reliable because cancer-linked DNA methylation patterns were relatively stable over time and DNA was considerably more stable than RNAs or proteins in archived materials [3]. The epigenetic marks also has advantages over the stable genetic alterations (e.g., somatic mutations, SCNVs, and SNPs) such as

tolerance of non-tumor cell contamination of samples, hints of tumor cells of origin, and allowance of a quantitative test [34]. Moreover, aberrant DNA methylation changes usually preceded genetic defects and abnormal expression, and represented very early events during carcinogenesis [35, 36]. The assessment of DNA methylation could render a more timely and accurate molecular profiling of a given tumor. Finally, the availability of drugs that reverse epigenetic modifications (e.g., DNA methyltransferase inhibitors, histone deacetylase inhibitors) makes DNA methylation analysis more therapeutically useful [3, 34]. Collectively all those advantages had made more appealing the development of a powerful DNA methylation signature for GBM prognostication.

In this study, by focusing on differential DNA methylation in GBMs, we developed a novel six-CpGs panel for prognostication. The six-CpGs signature had been demonstrated to be a robust and independent prognostic factor for GBMs, and was better than other molecular indicators such as G-CIMP status and proneural subtype. Another major advantage of the epigenetic signature is its biological implications. Among the locus-specific genes, *ADRA2C* and *TRIM58* were epigenetically silenced, and *TRIM38* and *MS4A7* were upregulated in GBMs. *ADRA2C* is a subtype of alpha-2-adrenergic receptors and has critical roles in normal brains function [37]. The dramatic decrease in *ADRA2C* expression indicated the disruption of normal brain function in GBMs. Interestingly; the other three transcriptionally altered genes were all related to immune system. *TRIM38* and *TRIM58* belong to the E3 ubiquitin ligase superfamily [37]. *TRIM38* was reported to be a negative regulator of innate immunity and inflammatory response [38-40]. *TRIM58* was involved in the regulation of pathogen-recognition and innate response [41]. *MS4A7* was associated with mature cellular function in the monocytic lineage [37]. Previous studies showed that

epigenetic modulation of immune-related genes is often taken advantage by neoplastic cells to promote immune escape by impairing their immunogenicity and immune recognition, and establishing immunosuppressive microenvironments [42]. In this study, we found that the defined risk subgroups were highly associated with differential enrichments in immune-relevant gene sets. Therefore, we proposed that the epigenetic panel may have implications in regulating GBM-specific immune response. Of note, two hypomethylated CpGs were not associated with apparent expression alteration in GBMs, but were essential for optimal prognostication. Recent studies suggested that, instead of a direct linkage to altered expression, cancer-specific DNA hypomethylation may also have functional impacts via contributing to disrupted heterochromatin, leading to loss of both epigenetic and transcriptional regulation, and resulting in hyper-variability of expression, and even have interactions with important genetic domains in cancers [36].

Bevacizumab has been the most promising anti-angiogenic agents for treating GBMs and especially recurrent cases [2]. Unfortunately two recent Phase III trials failed to yield clear OS benefits with the addition of bevacizumab to Stupp regimen in newly diagnosed GBMs, making more necessary the search of powerful predictive indicator for bevacizumab outcomes. [31, 32] Intriguingly, in this study, we observed the differential anigiogeneic profiles and survival outcomes of anti-angiogeneic therapy within each risk subgroup; high-risk patients seemed to benefit more from bevacizumab-contained therapy than low-risk ones. Therefore, the six-CpGs signature may have potential value to guide the usage of bevacizumab especially for high-risk patients, and thus be helpful for sparing low-risk ones who are molecularly unlikely to benefit from the aggressive therapy of higher cost and potential toxicity. Of note, the finding was encouraging but should be conservatively interpreted due to study

limitations (e.g., incomplete drug data, second-line bevacizumab in most cases, and retrospective design). Prospective validation in randomized trials of first-line bevacizumab will be needed for definitive conclusion.

The epigenetic signature also had potential to improve the current risk classification. The six-CpGs signature showed no discriminating value in the small subgroup of GBMs with G-CIMP (about 10%), characterized by mutations in *IDH* and favorable OS [25], as all G-CIMP+ tumors were low-risk. However, it was useful for identifying patients with different prognoses among the majority of GBMs without G-CIMP. The six-CpGs signature also showed great discriminating value in stratified RT/TMZ cohorts with each *MGMT* methylation status. *MGMT* methylation status had been by far the most informative biomarker for GBMs. However, its clinical value was much compromised due to lack of a direct linkage between *MGMT* testing and TMZ usage especially in unmethylated tumors [7]. Our six-CpGs signature could refine the *MGMT*-based risk classification, and be helpful for improving current clinical choice on TMZ for GBMs.

There have been fewer multi-maker epigenetic biomarkers for GBM prognostication. Shukla et al reported a nine-CpGs prognostic signature with implications of abnormal activation of NF-kB signaling [43]. Lai et al. reported a hypermethylated signature of human embryonic stem cell (hESC)-associated genes [15]. The signatures both had greatly expanded our knowledge of the epigenetic features for GBMs. Unfortunately they had limitations as clinically useful biomarkers in some crucial respects such as the employment of single discovery set with small sample size, the inclusion of CpGs associating SNPs, and the insufficient external validation. Our six-CpGs signature had been carefully developed with a particular focus on those issues. However limitations still existed in this study. First, the selection of prognostic CpGs was mainly focused

on CpGs that were differentially methylated in GBMs, which may result in the exclusion of other probes with high informative value. Second, our six-CpGs signature was more useful to identify a relatively small subset of clinically favorable patients, but showed limited capacity to provide information on the rest block of cases that are in the middle of the clinical spectrum. Third, despite that the six-CpGs signature showed robust prognostic value in G-CIMP- tumors, the model was not developed for that purpose. More powerful prognostic signatures for that tumor subset are still much needed and should be developed with exclusion of G-CIMP+ tumors. Finally lack of functional and mechanism studies hindered better application of the epigenetic biomarker.

Collectively our six-CpGs signature represented a promising tool for prognostication, and was of promising value for optimizing personalized management towards GBMs.

Acknowledgements

We gratefully acknowledge all the patients who agreed to participate in this study and to those who have provided their medical care. We gratefully acknowledge Pr Menei, Dr Le Reste, Dr. Vauleon, Dr. Quillien, and the Tumor Banks from Angers and Rennes for their constant support in the collection, processing and histological analysis of tumor samples. We also gratefully thank those who are willing to share their valuable scientific data (Prof. Rose K Lai for clinical data). I (A.Y.) thanks my fiancée (Dr. Yu Dong) for her great support and would you marry me? The results published here are in part based upon data generated by The Cancer Genome Atlas, German Cancer Research Center, and the research teams mentioned in our study. This work was supported by grants from National Natural Science Foundation of China

(No. 81402049, and No. 81471266) and by grants from the Brittany Region (France) et the FEDER (Europe).

References:

1. Wen PY and Kesari S, Malignant gliomas in adults. *N Engl J Med*. 2008;**359**: 492-507.
2. Yin AA, Cheng JX and Zhang X et al., The treatment of glioblastomas: a systematic update on clinical Phase III trials. *Crit Rev Oncol Hematol*. 2013;**87**: 265-82.
3. Issa JP, DNA methylation as a clinical marker in oncology. *J Clin Oncol*. 2012;**30**: 2566-68.
4. Baylin SB and Jones PA, A decade of exploring the cancer epigenome - biological and translational implications. *Nat Rev Cancer*. 2011;**11**: 726-34.
5. Rodriguez-Paredes M and Esteller M, Cancer epigenetics reaches mainstream oncology. *Nat Med*. 2011;**17**: 330-39.
6. Malzkorn B, Wolter M and Riemenschneider MJ et al., Unraveling the glioma epigenome: from molecular mechanisms to novel biomarkers and therapeutic targets. *Brain Pathol*. 2011;**21**: 619-32.
7. Yin AA, Zhang LH and Cheng JX et al., The predictive but not prognostic value of MGMT promoter methylation status in elderly glioblastoma patients: a meta-analysis. *PLoS One*. 2014;**9**: e85102.
8. Yin AA, Etcheverry A and He YL et al., Integrative analysis of novel hypomethylation and gene expression signatures in glioblastomas. *Oncotarget*. 2017;**8**: 89607-19.

9. Stupp R, Mason WP and van den Bent MJ et al., Radiotherapy plus concomitant and adjuvant temozolomide for glioblastoma. *N Engl J Med*. 2005;**352**: 987-96.

10. Altman DG, De Stavola BL and Love SB et al., Review of survival analyses published in cancer journals. *Br J Cancer*. 1995;**72**: 511-18.

11. Teschendorff AE, Marabita F and Lechner M et al., A beta-mixture quantile normalization method for correcting probe design bias in Illumina Infinium 450 k DNA methylation data. *Bioinformatics*. 2013;**29**: 189-96.

12. Etcheverry A, Aubry M and de Tayrac M et al., DNA methylation in glioblastoma: impact on gene expression and clinical outcome. *BMC Genomics*. 2010;**11**: 701.

13. Brennan CW, Verhaak RG and McKenna A et al., The somatic genomic landscape of glioblastoma. *Cell*. 2013;**155**: 462-77.

14. Zhang W, Yan W and You G et al., Genome-wide DNA methylation profiling identifies ALDH1A3 promoter methylation as a prognostic predictor in G-CIMP-primary glioblastoma. *Cancer Lett*. 2013;**328**: 120-25.

15. Lai RK, Chen Y and Guan X et al., Genome-wide methylation analyses in glioblastoma multiforme. *PLoS One*. 2014;**9**: e89376.

16. Kurscheid S, Bady P and Sciuscio D et al., Chromosome 7 gain and DNA hypermethylation at the HOXA10 locus are associated with expression of a stem cell related HOX-signature in glioblastoma. *Genome Biol*. 2015;**16**: 16.

17. Sturm D, Witt H and Hovestadt V et al., Hotspot mutations in H3F3A and IDH1 define distinct epigenetic and biological subgroups of glioblastoma. *Cancer Cell*. 2012;**22**: 425-37.

18. Johnson WE, Li C and Rabinovic A, Adjusting batch effects in microarray expression data using empirical Bayes methods. *Biostatistics*. 2007;**8**: 118-27.

19. Du P, Zhang X and Huang CC et al., Comparison of Beta-value and M-value methods for quantifying methylation levels by microarray analysis. *BMC Bioinformatics*. 2010;**11**: 587.

20. Hothorn T and Zeileis A, Generalized maximally selected statistics. *Biometrics*. 2008;**64**: 1263-69.

21. Madhavan S, Zenklusen JC and Kotliarov Y et al., Rembrandt: helping personalized medicine become a reality through integrative translational research. *Mol Cancer Res*. 2009;**7**: 157-67.

22. Gravendeel LA, Kouwenhoven MC and Gevaert O et al., Intrinsic gene expression profiles of gliomas are a better predictor of survival than histology. *Cancer Res*. 2009;**69**: 9065-72.

23. Subramanian A, Tamayo P and Mootha VK et al., Gene set enrichment analysis: a knowledge-based approach for interpreting genome-wide expression profiles. *Proc Natl Acad Sci U S A*. 2005;**102**: 15545-50.

24. Mermel CH, Schumacher SE and Hill B et al., GISTIC2.0 facilitates sensitive and confident localization of the targets of focal somatic copy-number alteration in human cancers. *Genome Biol*. 2011;**12**: R41.

25. Noushmehr H, Weisenberger DJ and Diefes K et al., Identification of a CpG island methylator phenotype that defines a distinct subgroup of glioma. *Cancer Cell*. 2010;**17**: 510-22.

26. Verhaak RG, Hoadley KA and Purdom E et al., Integrated genomic analysis identifies clinically relevant subtypes of glioblastoma characterized by abnormalities in PDGFRA, IDH1, EGFR, and NF1. *Cancer Cell*. 2010;**17**: 98-110.

27. Bady P, Sciuscio D and Diserens AC et al., MGMT methylation analysis of glioblastoma on the Infinium methylation BeadChip identifies two distinct CpG

regions associated with gene silencing and outcome, yielding a prediction model for comparisons across datasets, tumor grades, and CIMP-status. *Acta Neuropathol*. 2012;**124**: 547-60.

28. Macdonald DR, Cascino TL and Schold SJ et al., Response criteria for phase II studies of supratentorial malignant glioma. *J Clin Oncol*. 1990;**8**: 1277-80.
29. Heagerty PJ, Lumley T and Pepe MS, Time-dependent ROC curves for censored survival data and a diagnostic marker. *Biometrics*. 2000;**56**: 337-44.
30. Ceccarelli M, Barthel FP and Malta TM et al., Molecular Profiling Reveals Biologically Discrete Subsets and Pathways of Progression in Diffuse Glioma. *Cell*. 2016;**164**: 550-63.
31. Chinot OL, Wick W and Mason W et al., Bevacizumab plus radiotherapy-temozolomide for newly diagnosed glioblastoma. *N Engl J Med*. 2014;**370**: 709-22.
32. Gilbert MR, Dignam JJ and Armstrong TS et al., A randomized trial of bevacizumab for newly diagnosed glioblastoma. *N Engl J Med*. 2014;**370**: 699-708.
33. Roychowdhury S and Chinnaiyan AM, Translating cancer genomes and transcriptomes for precision oncology. *CA Cancer J Clin*. 2016;**66**: 75-88.
34. Zhu J and Yao X, Use of DNA methylation for cancer detection: promises and challenges. *Int J Biochem Cell Biol*. 2009;**41**: 147-54.
35. Fleischer T, Frigessi A and Johnson KC et al., Genome-wide DNA methylation profiles in progression to in situ and invasive carcinoma of the breast with impact on gene transcription and prognosis. *Genome Biol*. 2014;**15**: 435.

36. Timp W, Bravo HC and McDonald OG et al., Large hypomethylated blocks as a universal defining epigenetic alteration in human solid tumors. *Genome Med*. 2014;**6**: 61.

37. Pruitt KD, Tatusova T and Brown GR et al., NCBI Reference Sequences (RefSeq): current status, new features and genome annotation policy. *Nucleic Acids Res*. 2012;**40**: D130-35.

38. Hu MM, Xie XQ and Yang Q et al., TRIM38 Negatively Regulates TLR3/4-Mediated Innate Immune and Inflammatory Responses by Two Sequential and Distinct Mechanisms. *J Immunol*. 2015;**195**: 4415-25.

39. Hu MM, Yang Q and Zhang J et al., TRIM38 inhibits TNFalpha- and IL-1beta-triggered NF-kappaB activation by mediating lysosome-dependent degradation of TAB2/3. *Proc Natl Acad Sci U S A*. 2014;**111**: 1509-14.

40. Zhao W, Wang L and Zhang M et al., Tripartite motif-containing protein 38 negatively regulates TLR3/4- and RIG-I-mediated IFN-beta production and antiviral response by targeting NAP1. *J Immunol*. 2012;**188**: 5311-18.

41. Thom CS, Traxler EA and Khandros E et al., Trim58 degrades Dynein and regulates terminal erythropoiesis. *Dev Cell*. 2014;**30**: 688-700.

42. Maio M, Covre A and Fratta E et al., Molecular Pathways: At the Crossroads of Cancer Epigenetics and Immunotherapy. *Clin Cancer Res*. 2015;**21**: 4040-47.

43. Shukla S, Pia PI and Thinagararjan S et al., A DNA methylation prognostic signature of glioblastoma: identification of NPTX2-PTEN-NF-kappaB nexus. *Cancer Res*. 2013;**73**: 6563-73.

Legends for Figures

Figure 1: The development of the six-CpGs prognostic signature; (a) The study workflow for the risk-score signature construction; (b) Hierarchical clustering on the 508 CpGs that were commonly identified in all the three discovery sets accurately distinguished GBMs from non-tumor brain tissues in two discovery sets (RAUH_27k and GSE50923_27k) and an independent validation set (GSE60274_450k), with the similarity metric "Euclidean distance" and the clustering method "Centroid linkage"; TCGA_27k was not tested due to too few non-tumor controls (n=4) relative to the large number of GBMs (n=282); (c) the characteristics of the six-CpGs panel; open sea loci refer to CpGs that are more than 4000 bp away from CpGs island; (d) the DNA methylation of the six CpGs and the expression levels of the relevant genes between GBMs (n=279) and non-tumor brain tissues (n=10) from TCGA_27k; P values for wilcoxon sum rank test and standard t test were respectively indicated for DNA methylation and expression data.

Figure 2: The prognostic performance of the six-CpGs signature on overall survival (a) in the pooled discovery cohorts (*left*) and each discovery set (*right*); and (b) in the pooled validation cohorts (*left*) and each validation set (*right*); p-values from log-rank test and meta-analysis were indicated ; RT=radiation, TMZ=temozolomide

Figure 3: Molecular characterization of the six-CpGs signature using the multi-dimensional TCGA data; (a) heat maps of methylation levels of the six CpGs; each row represents a CpGs; each column represents a sample which is ordered by the assigned risk scores; patient age, clinical features, molecular subgroups, copy number variations and mutational status are indicated for each sample (n=395); regarding distribution, p-values for chi-square or fisher's exact tests were indicated; * indicated

significant distribution features event after excluding G-CIMP+ tumors; (b) GSEA enrichment plots of representative gene sets for low-risk and high-risk tumors; (c) the potential links of the defined risk subgroups to differential outcomes of bevacizumab in patients with combination of RT and TMZ; the usage of bevacizumab conferred a clear benefit in OS and especially short-term survival to high-risk patients, but appeared to be associated with similar OS in low-risk ones in TCGA_27k/450k (either first-line or at progression; *upper panel*), GSE50923_27k (at progression; middle panel) and RAUH_27k/450k (at progression; *bottom panel*); secondary, recurrent and treated samples from TCGA were excluded for this analysis; (d) meta-analysis of each cohort confirmed the differential bevacizumab outcomes with respect to each risk subgroup by yielding a significant result for subgroup difference test (P=0.03); Bev=bevacizumab

Figure 4: The prognostic performance of the six-CpGs signature in stratified cohorts by known epigenetic biomarkers; (a) risk classification of the six-CpGs signature and G-CIMP status in a pooled survival analysis of all available patients; p-values from meta-analysis <0.01 for each pair-wise comparison; (b) risk classification of the six-CpGs signature and G-CIMP status in a pooled survival analysis of all available patients with combination of RT and TMZ; p-values from meta-analysis <0.01 for each pair-wise comparison, except for the comparison of low-risk and *MGMT* unmethylated tumors vs. high-risk and unmethylated ones (p=0.540)

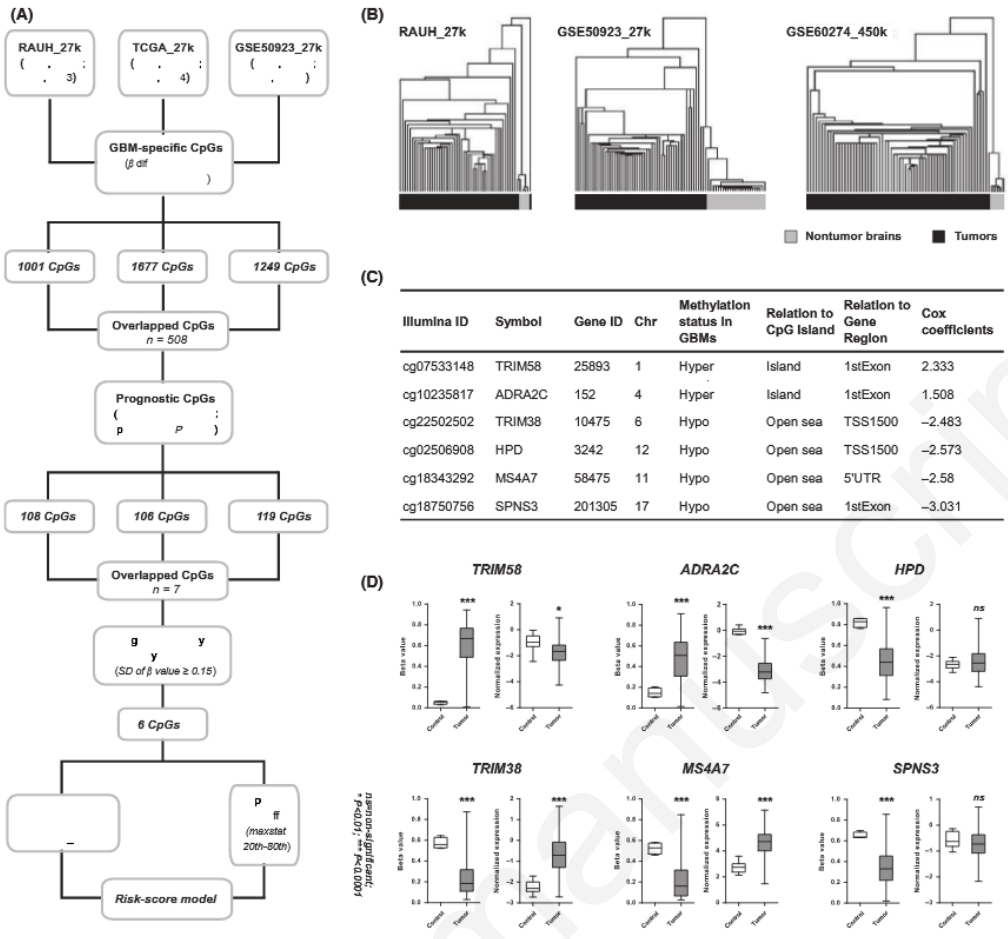

(C)

Illumina ID	Symbol	Gene ID	Chr	Methylation status in GBMs	Relation to CpG Island	Relation to Gene Region	Cox coefficients
cg07533148	TRIM58	25893	1	Hyper	Island	1stExon	2.333
cg10235817	ADRA2C	152	4	Hyper	Island	1stExon	1.508
cg22502502	TRIM38	10475	6	Hypo	Open sea	TSS1500	–2.483
cg02506908	HPD	3242	12	Hypo	Open sea	TSS1500	–2.573
cg18343292	MS4A7	58475	11	Hypo	Open sea	5'UTR	–2.58
cg18750756	SPNS3	201305	17	Hypo	Open sea	1stExon	–3.031